Martian Environmental Chamber: Dust System Injection

F. Cozzolino[1], V.Mennella[1], A.C.Ruggeri[1], G.Mongelluzzo[1,2],G.Franzese[1], C. I. Popa[1], C. Molfese[1], F. Esposito[1], C.Porto[1], D.Scaccabarozzi[3].

Affiliations

[1] INAF – Osservatorio Astronomico di Capodimonte, Salita Moiariello 16, 80131 Napoli, Italy.

[2] Department of Industrial Engineering, University of Naples "Federico II", Piazzale Tecchio 80, 80125 Napoli, Italy

[3] Department of Mechanical Engineering Politecnico of Milano, via Gaetano Previati, 1/c, 23900 , Lecco, Italy

Abstract

The aim of this work is to describe the development and implementation of an experimental setup able to reproduce some characteristics of the Martian atmosphere. The development of such setup fits into the context of MicroMED project, that foresees the development of an optical particle counter to be accommodated on the ExoMars 2020 Surface Platform, as part of the suite of sensors named Dust Complex.

MicroMED will perform the first direct measurement of the size distribution of the powder close to Martian surface. The experimental setup is able to reproduce the characteristics of the Martian atmosphere: pressure, atmospheric composition, the actual temperature in which MicroMED will operate (from -20 °C to 40 °C) and the most important thing: *the presence of suspended dust*.

The main result obtained in this work was to have found the right configuration of an experimental setup in which to test sensors or instruments that work in Martian conditions. In particular, a dust injection system has been developed in order to obtain a dust distribution without aggregations and localized for a correct calibration of the instrument.

Keywords

Dust, Mars, Injection, Airborn Dust , MicroMED ExoMars, Martian Atmosphere, Particle Counter.

1. Introduction

Dust on Mars for years now has stirred the interest of the scientific community being it the protagonist of many phenomena observed on the planet, for example dust absorbs and scatters solar radiation, strongly modifying atmospheric thermal structure and balance. But the most spectacular events that are observed on Mars, where dust is the main actress, are local and global sandstorms and dust devils. The mechanisms of , transport and distribution of these phenomena are not yet well determined by the models (Kahre, 2006; Newman at al. 2002; Taylor, 2007) because, unfortunately, there is a lack of information on the physical characteristics of the grains such as size distribution and concentration. The only information available to date on physical characteristics of the powder has been provided by light absorbance measurements. Indeed, measuring the optical depth with complex calculations and making strong assumptions on the shape, on the refractive index of the particles, it is possible to obtain the effective radius of the airborn dust distribution.

Currently, there are different observations of the dust haze, performed using both the surface and orbital images (Toon et al., 1977; Drossart et al., 1991; Pollack et al., 1995; Tomasko et al, 1999; Greeley et al., 2006; Vasilyev et al., 2009; Fedorova et al., 2009; Vicente-Retortillo, et al., 2017). Currently, a direct study of the airborne dust has not been performed yet.

To provide a direct measurement of airborne dust, has been developed MicroMED (ScaccabarozziDiego et al 2018) , an optical particles counter capable of operating in Martian atmospheric conditions which was then selected for ExoMars 2020 Mission, onboard of the Surface Platform. MicroMED is an optical particle counter based on the light diffusion principle and is able to aspire the dust and analyze the light scattered from the single grains to measure their size and

abundance. It will operate directly close to the surface, where dust is lifted, allowing monitoring of the dust injection into the atmosphere. MicroMED is part of the Dust Complex, a suite of five sensors devoted to the study of Martian dust. Apart from MicroMED, the suite is composed by: Conductivity Sensor, Impact Sensor, Electric Probes and EM-sensor in order to study the other events linked to the lifted dust for example the electrical field. Indeed, airborne dust tends to acquire charge for triboeletrification, the process depends on the grains composition and size (Kunkel, 1950; McCarty and Whitesides, 2008; Melnik and Parrot, 1998; Desch and Cuzzi, 2000), as well on the environmental conditions (Esposito et al., 2016, Harrison et al. 2016; Neakrase et al., 2016; Murphy et al., 2016). Dust charging can lead to strong electric field, in theory able to overcome the Martian electric breakdown (Farrell et al., 2017; Franzese et al., 2018).

In order to verify the performances and calibrate MicroMED, it was necessary to recreate the atmospheric conditions that the instrument will find on Mars, in particular the presence of dusts. The response of MicroMED to this condition has been simulated using a CFD (Computational Fluid Dynamics) analysis in order to understand what are the critical parameters and the range of variation that have to be guaranteed in laboratory (Mongelluzzo et al. 2018). In order to reproduce the Martian conditions, a simulator chamber has been developed in which it is possible to recreate the Mars atmospheric composition, pressure, temperature and dust concentration that MicroMED will face during its operative time. Obviously, this type of setup can be used for the calibration of different instruments such as impact sensors, microbalances and optical particle counters.

2. Mars Atmosphere Simulator

To recreate the atmospheric conditions of Mars in which is possible to verify the performances of MicroMED, a cylindrical vacuum chamber has been used, called simulation chamber, as shown in Figure 1 Vacuum chamber to simulate the Martian atmosphere.

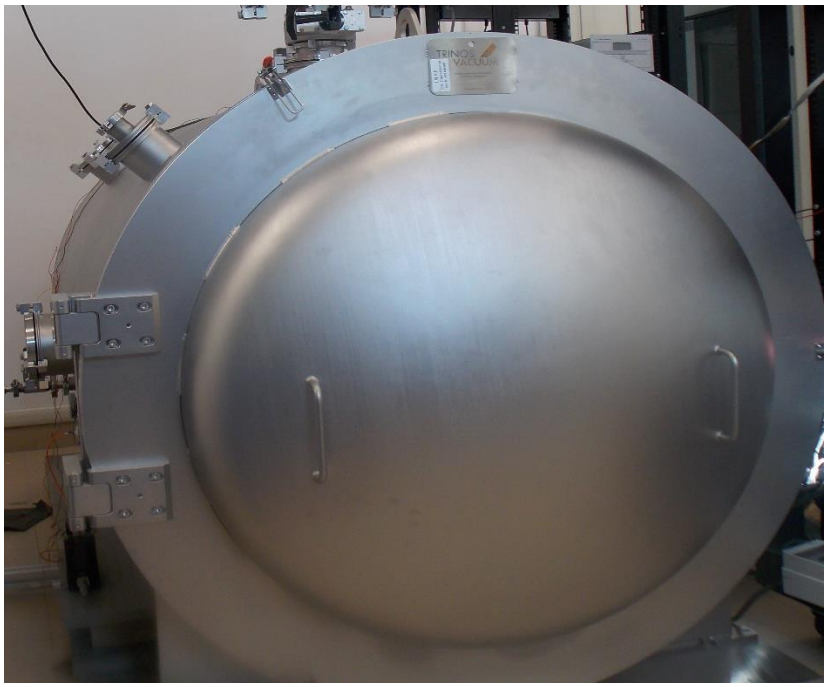

Figure 1 Vacuum chamber to simulate the Martian atmosphere

The average pressure on Mars is around 7 - 8 mbar (Zurek et al. 1992; Martinez G.M, et al. 2017). This value was obtained in the simulation chamber, using a pumping system consisting of two cascade pumps: a Varian Tri_Scroll 600 Series Dry Scroll and a Turbo V-750 Twis Torr. The pumping system can generate a maximum vacuum of about 10^{-4} mbar in the chamber, therefore suitable for reproducing the Martian pressure regime. The Scroll pump is also equipped with a VPI valve that blocks the flow in the direction of the pump when it stops functioning. Pressure monitoring is performed through the Pfeiffer compact capacitance gauge with a measurement range of 0-1000 mbar. The sensor is connected to an external controller that displays the value of the pressure in the chamber.

In prevision of a MicroMED testing campaign, the chamber had to allow the injection of dust grains of different sizes. In particular, in order to test the response of the instrument to calibrated monodispersed grains, these have to remain separated from others. . Indeed, the electrification of the grains could lead to the formation of aggregates, that in turn alter the size distribution in input introducing a further level of uncertain.

An injection system has been realized capable of injecting a flow of thousands of separated grains inside the chamber. The injection system had been developed and improved through several intermediate steps, before obtaining the desired performance.

3. Dry Injection System

The first injection system, named Dry Injection, was made up of a holder containing the dry particles, connected to the chamber through a gate valve. When the valve is opened, due to the pressure difference between the holder (ambient pressure) and the chamber (1 mbar), the particles are aspired into the chamber.

This injection system shows two problems:

1) *The flux of particles is focused in a very restricted area inside the chamber, so it is not uniformly distributed*.

2*) The formation of groups of aggregated particles that represents a critical issue for the calibration of the MicroMED optical particle counter.*

In order to verify the reliability of the system, several tests have been performed. To monitor the distribution of grains inside the chamber, several aluminum stubs have been deployed on its base as shown in Figure 2. Each stub was covered with an adhesive carbon disc on which the injected particles could sediment. All carbon discs were then analyzed with a Scanning Electronic Microscope (SEM).

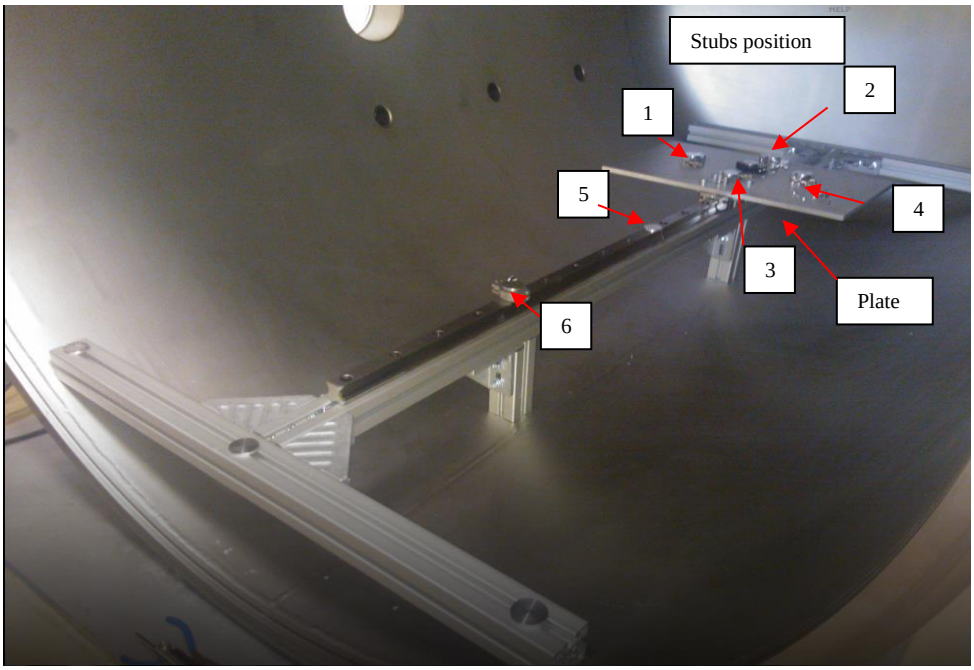

Figure 2 Aluminum Stub with Carbon Disc inside the simulation chamber in order to verify the particles distribution

.

Some samples, observed at the SEM, are shown in Figure 3 (single aggregate) and **Figure 4**(multiple aggregates) . It is evident the formation of particles aggregates using a dry injection system .

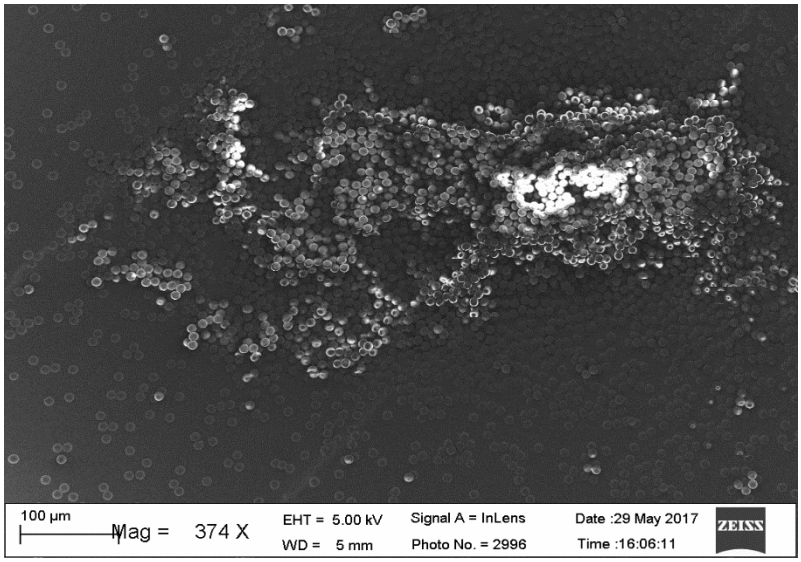

Figure 3 Local concentration of particles injected with dry system as observed over carbon stubs at the SEM. Details of SEM. Parameters : Mag = Magnification, WD = Work Distance, EHT = Power Supply of Gun, Scale Bar = 100 µm

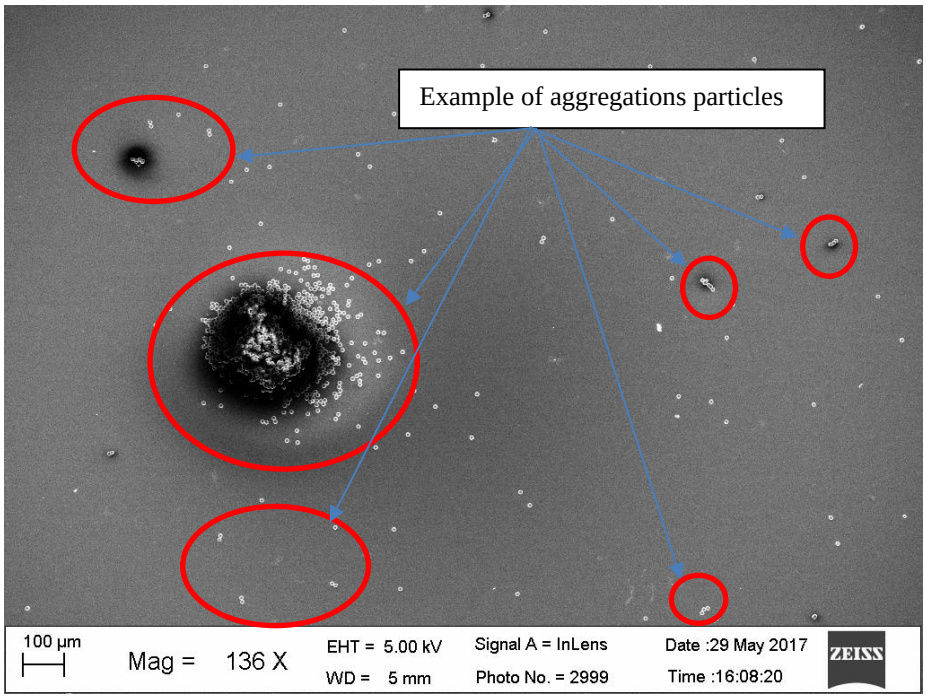

Figure 4 Several **e**vidence of particles aggregation in the chamber after injection of dry particles. Details of SEM. Parameters : Mag = Magnification, WD = Work Distance, EHT = Power Supply of Gun,
Scale Bar = 100 µm

4. "Wet" Injection System

In order to solve the problem of the particle aggregates presented in the Dry Injection System, a different injection system has been developed, using grains embedded in a solution.

The system shown in Figure 5 is constituted by a dispenser (Grimm Aerosol Dispensers mod 7811), a second vacuum cylindrical chamber (pre-chamber), considerably smaller than the Martian vacuum chamber, and a gate valve.

The used aerosol generator, is shown in Figure 6. It nebulizes a solution consisting of water and particles to be injected into the pre-chamber. The nebulization is the reduction of a liquid in very

small parts (drops), which is obtained, for example, by colliding the liquid with a jet of air at high speed, or forcing the liquid to pass through a very narrow orifice.

The solution before to be nebulized is placed in an ultrasonic chamber in order to well separate the embedded grains.

Nebulizer flow rate is adjustable. The maximum flow rate is 7 l /min and is reachable at 1 atm pressure. For our tests we set the flow rate at 7 l/min. The features of dispenser are summarized in Table 1.

Supply Voltage	240 V	Aerosol Substance	Aqueous solutions
Frequency	50 to 60 Hz	Nebulizer flow rate	2.5 to 7.0 [l/min]
Maximum current	1.7 A	Dryer flow rate	7.5 to 17 [l/min]
Temperature Range	0 [°C] to 40 [°C]	Nebulizer liquid capacity	3 to 10 [ml]
Aerosol output air pressure range	Equal to atmospheric pressure	Particle concentration	$\geq 10^7$ [1/cm^3]

Table 1 Features of Grimm mod 7.811 Particle-Generator

The pre-chamber, has dimensions of 30 cm in diameter x 25 cm in height. The injection system is connected to the top of the first chamber. Between the second and the first chamber there is the gate valve as shown in Figure 5. The gate valve is operated by hand.

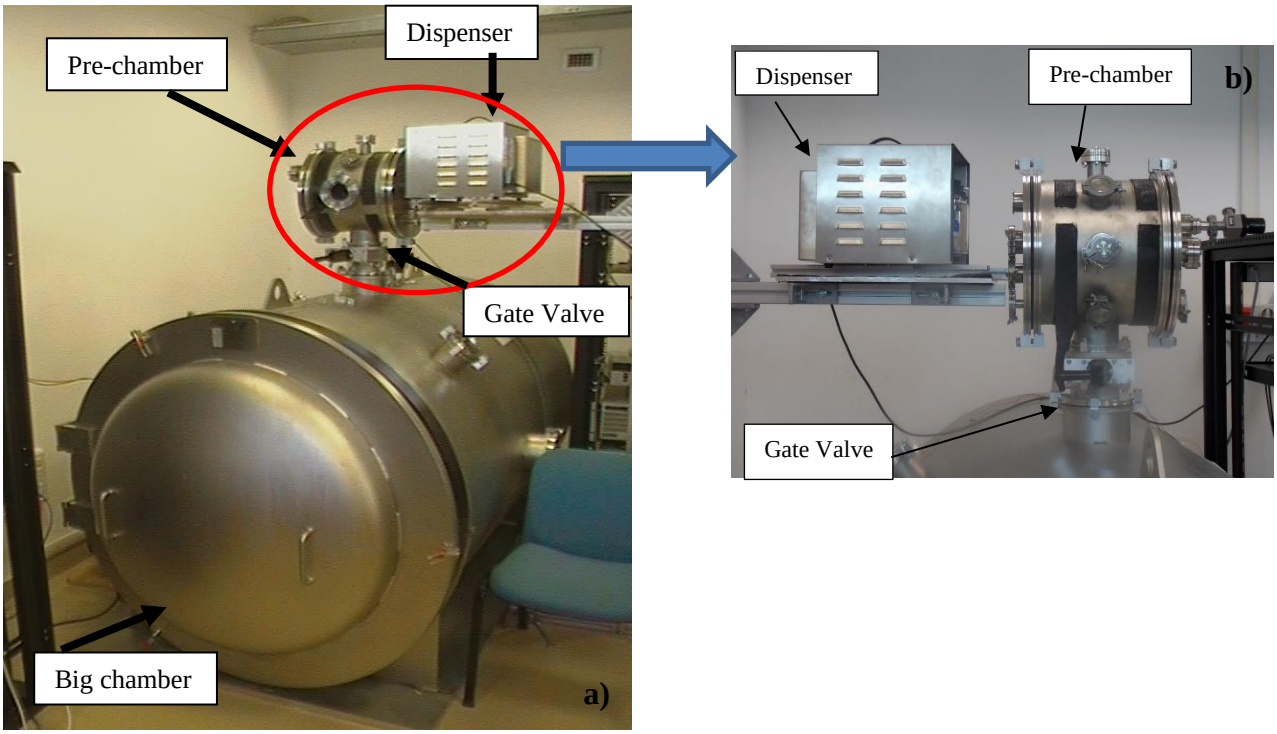

Figure 5 Martian Simulation chamber. **a)** The complete system; **b)** "Wet" injection system.

.

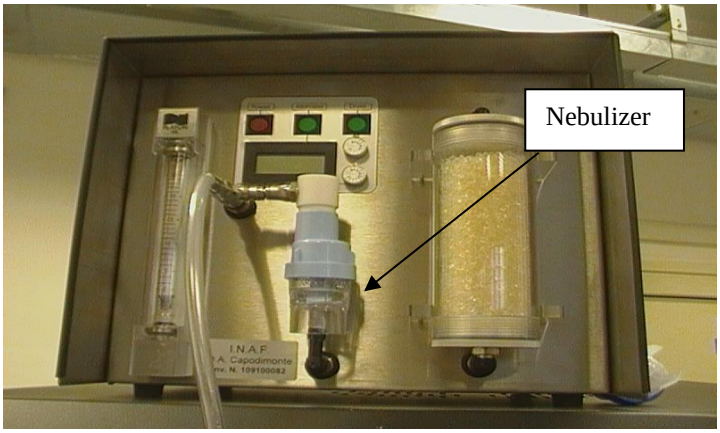

Figure 6 Particle Generator Model 7.811

4.1 Vacuum Pre-chamber

The vacuum pre-chamber (Figure 7) is a steel cylinder and it has 4 flanges, 3 DN 40 and DN 15 1 on upper base,; on its side there are 4 flanges DN 40 and 2 DN 100 . On the lower base there are 3 flanges DN 40 and 1 DN 15 flange. All flanges are Iso K. The flanges which will be used are: 1 DN 15 on the upper base of which will be connected to the output of the aerosol generator, 1 DN 100 where the valve will be connected manual gate and a flange reducing DN100-DN 15 on which connect the pipe coming from the large chamber (Martian Simulation Chamber). The rest of the flanges will be closed with blind flanges.

The pressure in the pre-chamber will be 1 atm as required by the characteristics of the particle generator.

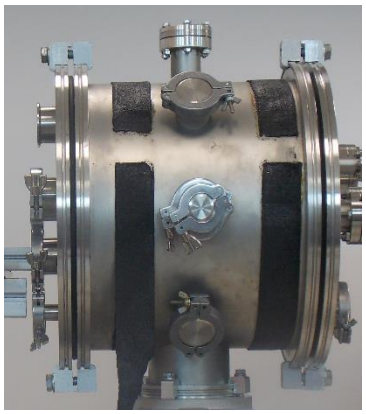

Figure 7 Vacuum Pre-Chamber

4.2 Big Vacuum Chamber (Martian Simulation Chamber)

The big vacuum chamber, where MicroMED will be tested, is a steel cylinder with 1,34 m in diameter and 2,05 m in length. It is provided on the upper part of a window DN 160 and three flanges DN 15 to one of which will be connected to the pipe coming from the pre-chamber. At theside there are 2 windows DN 160, 3 flanges DN 60, one of which will be used to feedthrough liquids for a future cooling system, 2 flanges DN 100 to one of which will be connected with a flange feedthrough that

will allow us to power with 6 V the MicroMED pump from the outside. The internal pressure will be increased to 6 mbar using a scroll pump Agilent mod TS600 220V 1 Ph. The chamber is provided of an internal moving aluminum panel that can slide on a track system in order to set its position. During the phase of testing, MicroMED will be placed on this base. The vacuum chamber is connected to the vacuum pre-chamber by a steel tube, which will guide the passage of the particles in the main chamber.

5. Measurements of particle distribution in Martian simulation chamber

Once the Simulator Chamber was implemented, a series of measurements were carried out to verify the functionality of the injection system and the distribution of the particles in the simulation chamber. Aluminum stubs have been positioned same as above mentioned (Figure 2). The injection system generates an aerosol of particles that is distributed inside the pre-chamber.

When the gate is opened, due to the difference in pressure between the simulation chamber (1 mbar) and pre-chamber (1 atm) the particles are sucked with high speed into the simulation chamber. The particles bounce on the bottom of the chamber and are spread. Once the equilibrium condition of 6 mbar is reached, the bounced particles deposit for gravity on the discs positioned at the base of the chamber. At the end of the settling process the discs are analyzed with the SEM. The disks have been numbered, each corresponding to a precise position within the chamber. At the end of the settling process the disks are analyzed with the SEM. The disks have been numbered, each corresponding to a precise position within the chamber. In particular, the disks 3, 4, and 5 have been positioned at the gate valve which represents the entry of the particles in the simulation chamber. The disks 1, 2 and 6 have been positioned respectively at one meter from the disk 3, at 0.7 meters from disk 3 and 0.15 cm from disk 5.

The test was performed using monodispersed particles with size 0.5, 1.30, 2.8, 4.32, 6.36, 8.43, 11, 14.98 µm. The same set of particles has been used during the calibration of MicroMED. From the analysis of the stubs to the SEM it is evident that injecting the particles with this injection system

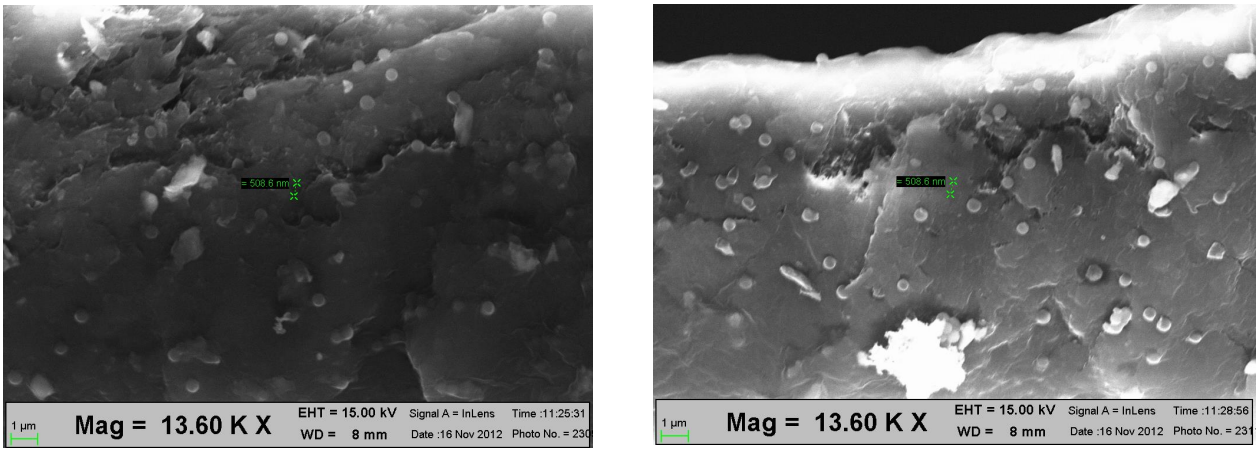

Figure 8 Absence of aggregates particels injected with the Wet Injection System disk 3 (on the right) and disk 5 (on the left). The green marker shows the size of particles, it is 508.6 nm

avoids the formation of the aggregates of particles how shown in Figure 8that were present with the dry injection system.

The results about distribution particles inside the big chamber are shown in Figure 9, where is shown the trend of the numerical density of the particles as a function of the position of the disks, for each used particle size.

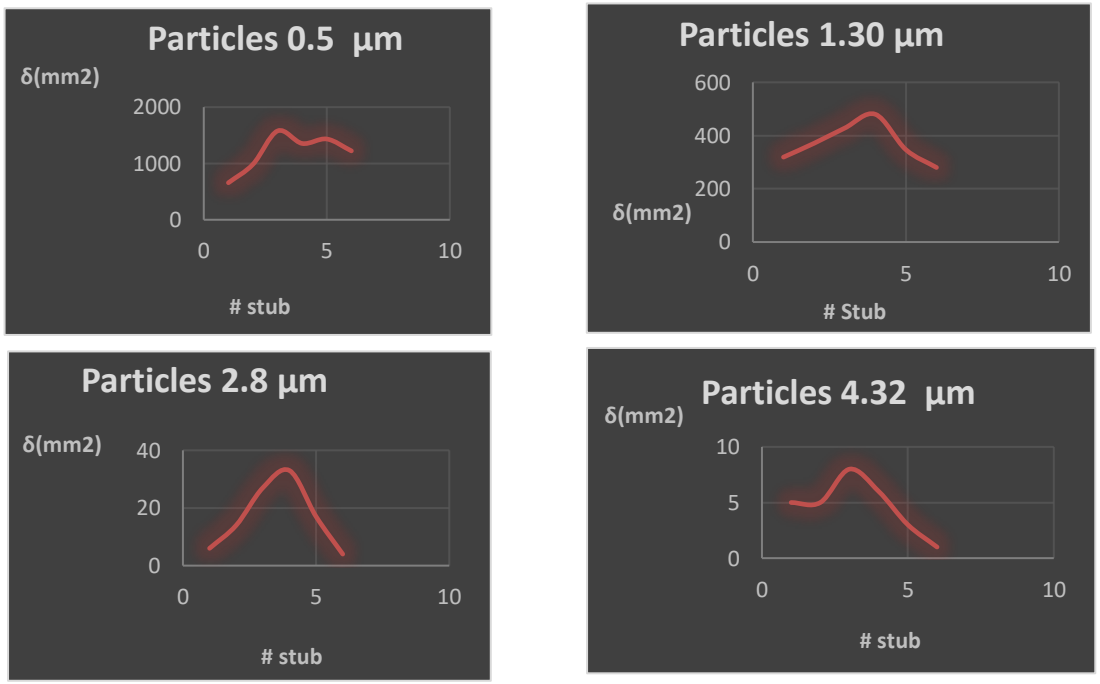

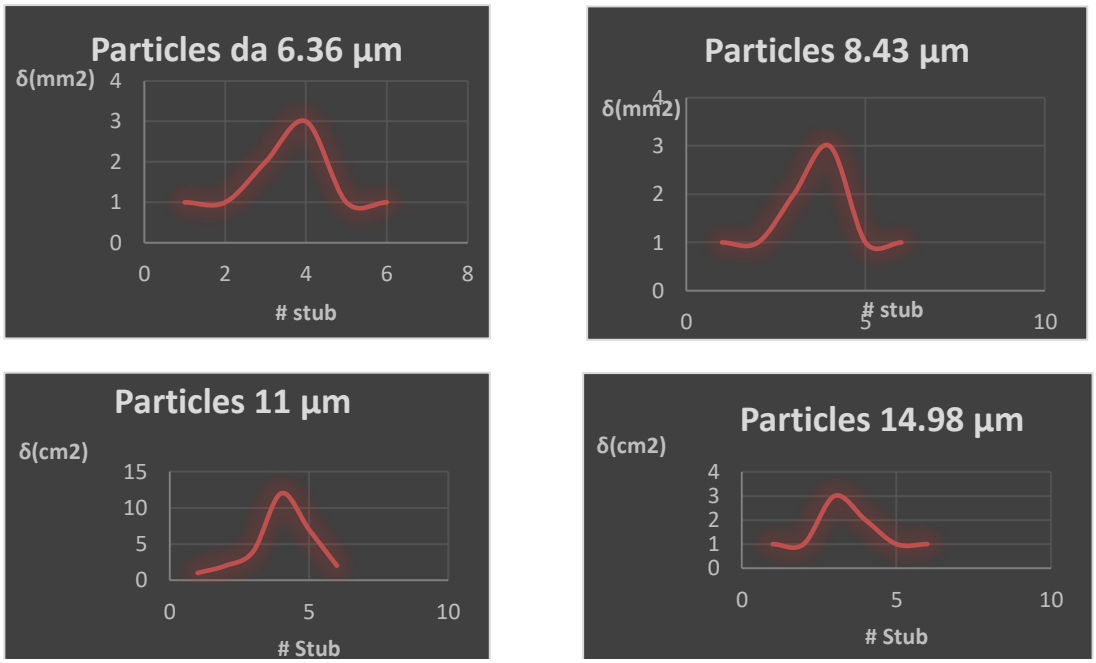

Figure 9 Particle distribution according to the position of the sampling discs positioned in the simulation chamber. Y-axis shows the density value, while x-axis the position of the disks

.

The plots show that the "wet" injection is able well spread into the simulation chamber the dust grains on the whole size range considered. The smaller particles tend to disperse more, distributing almost uniformly throughout the chamber, while the larger diameter particles tend to be distributed in the region corresponding to their entrance area (the area under the gate valve).

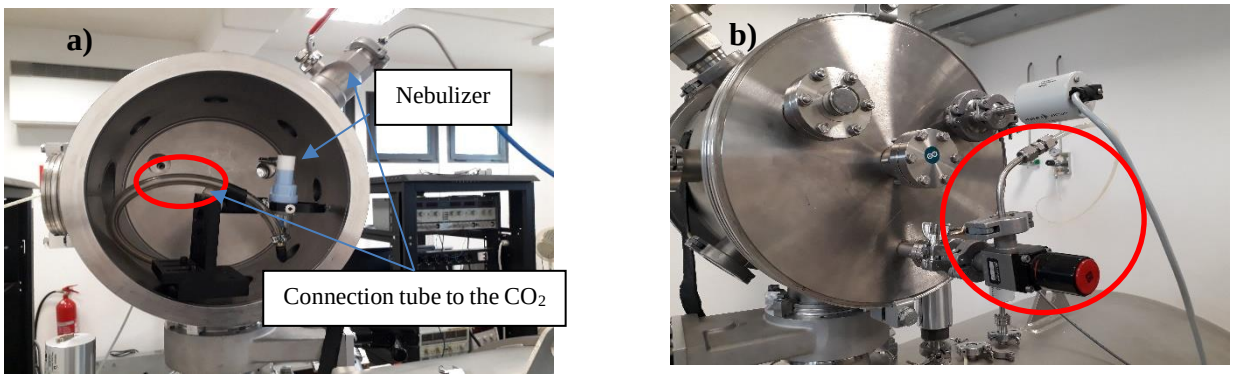

Figure 10 a) Nebulizer inside the pre-chamber connected to system injected of CO_2 **b)** System injected of CO_2

The injection system that makes use of the dispenser has a limitation, because it only works in presence of 1 bar atmosphere, so it can inject particles into the pre-chamber only if it has a pressure

of 1 bar. The consequence of this is that when the gate valve between the pre-chamber and the simulation chamber is opened, a strong pressure difference causes the particles to acquire a very high speed, so to bounce on the chamber bases and wall before being sampled by MicroMED. This causes a large dispersion and loss of particles. To improve this aspect, it has been simplified the particle injection system to control the input velocity of the particles in the simulation chamber. As shown in Figure 10, the Grimm dispenser was removed and just the nebulizer was placed, filled up with a solution of ethanol and particles, inside the pre-chamber connecting it to the CO_2 (Figure 10) injection system of the chamber. This configuration allows to inject the particles after having depressurized the pre-chamber (for example, bringing it to 15 - 16 mbar) with a pump, in order to control the pressure gap between the two chambers, as well as the particle velocity.

We used the ethanol instead of water for the particles solution in order avoid the freezing during the rapid gas expansion experienced caused by the gate opening. Ethanol is a very volatile liquid which evaporates at a pressure of 6 mbar and with a temperature of about 22°C, depositing on the walls of the chamber. Several measurements were made by injecting only ethanol to understand if the droplets that are generated could somehow be sucked. Test results show that MicroMED does not reveal ethanol.

6 MicroMED BreadBoard performance test

Using the results presented in the last section, it was possible to identify the optimal position where the grains concentration peaks. In this position, corresponding to the disks 3 and 4, we installed a BreadBoard version of MicroMED, as shown in Figure 11, in order to perform the first tests of the sensor performances.

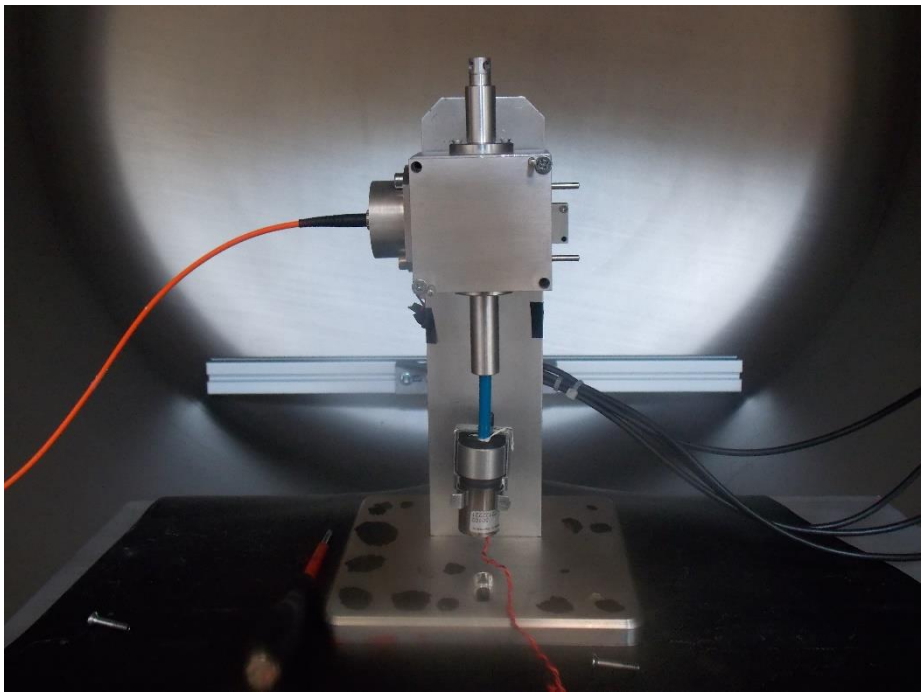

Figure 11 BreadBoard version of MicroMED installed in the simulation chamber

The tests performed with the upgraded injection system showed an increase in the number of particles acquired by MicroMED.

Table 2 shows the average amplitude values of the signals generated by the particles sucked by MicroMED, for grain size of 0.448, 1.046, 4.051, 8.496 micrometers. The particle signals were acquired using an electronic board having two channels with different amplification stage called Low and High. The Low channel was used for the study of the signals of the particles with a diameter greater than 2 microns and had an amplification factor of 10^5, while the High channel was used for the study of the signals of the particles with a diameter less than 2 microns and had the amplification factor of 10^7.

An example of the signals acquired by MicroMED BreadBoard in both channels are shown in Figure 12

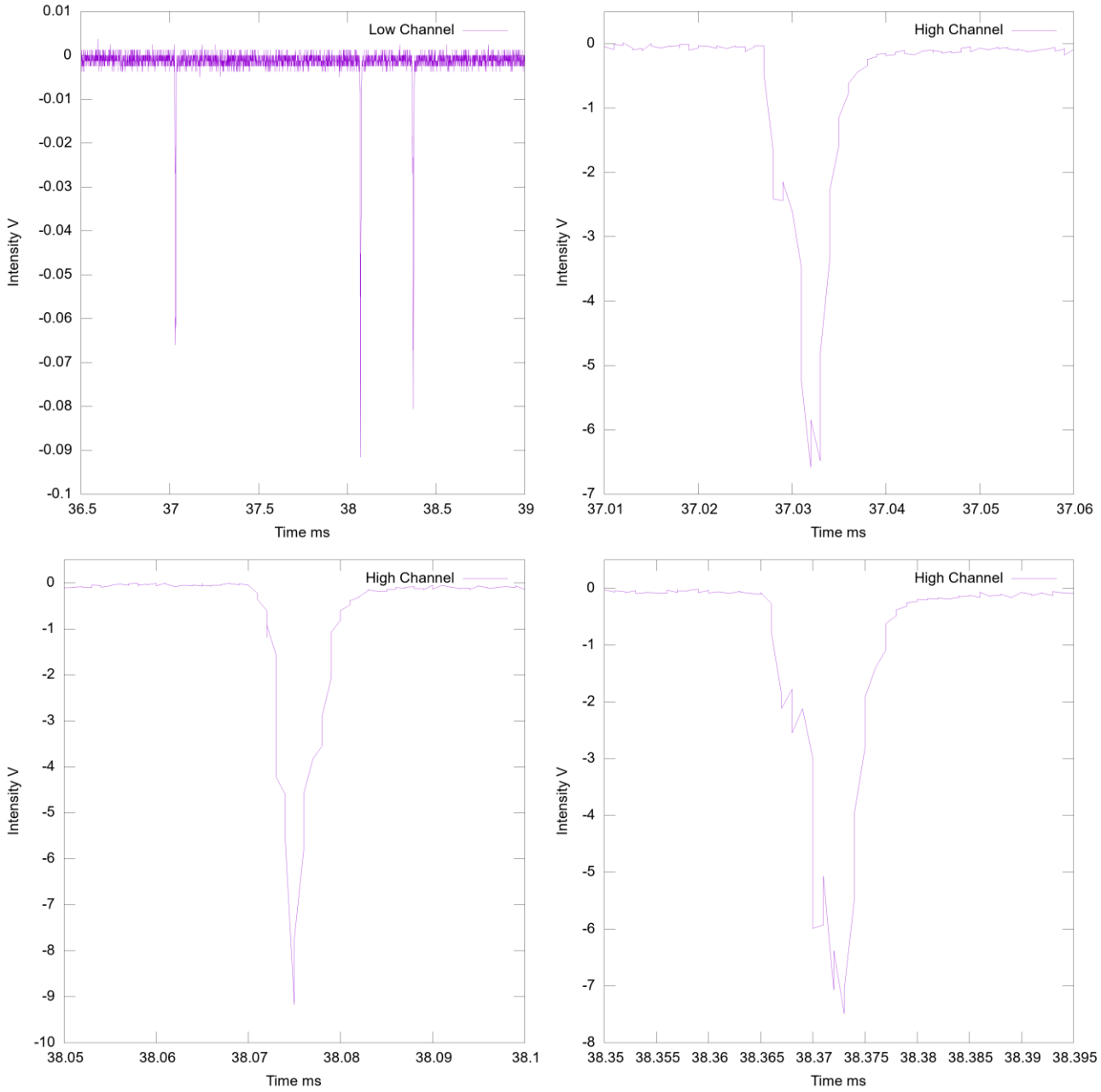

Figure 12 Example of the signals acquired by MicroMED BreadBoard. The first plot on top left shows an extract of the time series acquired in Low channel during the particles injection: three passing grains are visible. The successive plots show a zoom of these three signals in High channel.

Channel	Size (µm)	Number Signals	Mean (V)	Median (V)	Standard Deviation (V)	Lower Quartile (V)	Upper Quartile (V)
High	0.448	150	0.18	0.17	0.09	0.11	0.25
High	1.046	113	2.4	1.9	1.7	1.2	3.4

Low	4.051	135	0.18	0.15	0.19	0.09	0.20
Low	8.496	145	0.47	0.29	0.49	0.18	0.52

Table 2 The results in volt of the MicroMED BreadBoard acquisitions for the test with monodispersed spherical grains.

.

In Figure 13 two amplitude distribution of signals for High and Low channels are shown.

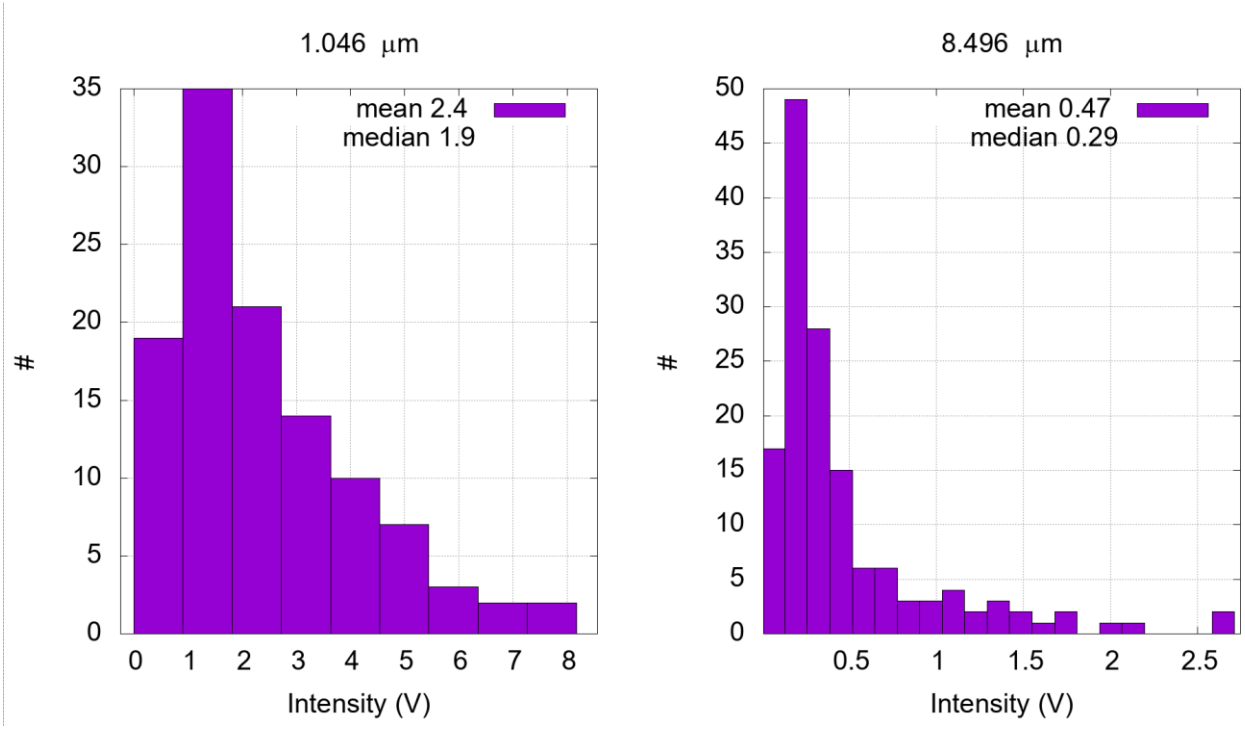

Figure 13 Intensity distribution of the signals acquired in by MicroMED BreadBoard: left) High Channel for the injection of a monodispersed samples of 1.046 micron spherical grains; right) Low Channel for the injection of a monodispersed samples of 8.496 micron spherical grains.

The average values of the amplitudes, shown in Table 2, were compared with the theoretical instrumental response of MicroMED, obtained from the Mie model. A good agreement between the theoretical and experimental trend can be seen in Figure 14.

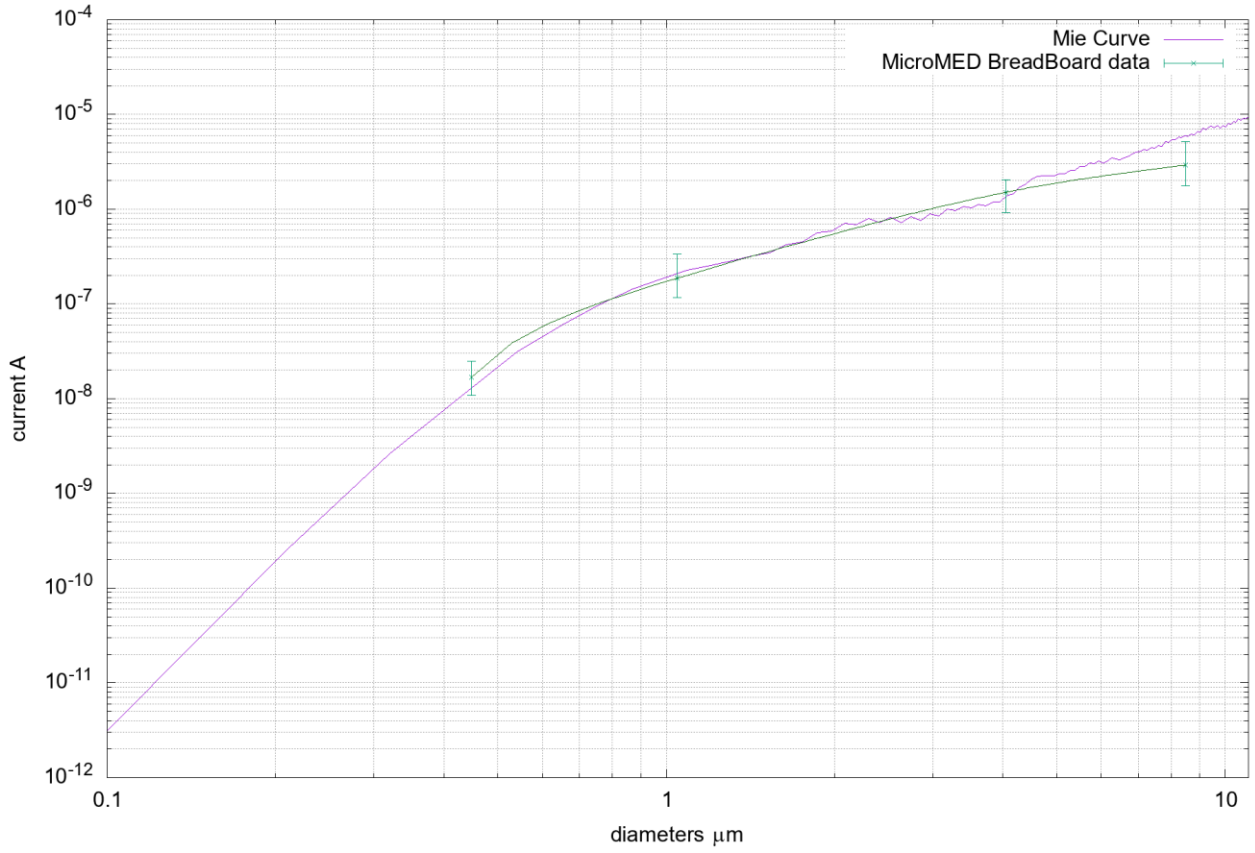

Figure 14 Comparison of the signals current obtained from the MicroMED BreadBoard measurements and the average theoretical Mie curve expected.

7. Conclusions

The next ESA/Roscosmos ExoMARS 2020 missions aim to investigate possible life traces on the Martian surface and study the Martian past and present climate, in order to address its sustainability for the life. To achieve this goal, it is fundamental to perform a proper characterization of the atmospheric dust and its interactions with the Martian weather.

MicroMED is an optical particle counter on board of the surface lander, as part of the Dust Complex, a suite of instruments aimed to the study of the characteristics of the primary lifted dust. In particular, MicroMED will acquire the first direct measurement of the primary dust amount and size distribution.

In order to develop the instrument, we realized a Martian simulation chamber able to reproduce the environment where MicroMED will operate. Here, the most important goal reached has been the

development of the correct configuration of the injection dust system, in order to obtain a dust distribution without aggregations and localized near the instrument.

The Dust Injection System is constituted by a system of vacuum chambers that allows the injection of dust particles in a controlled CO_2 low pressure environment. We decided to inject the dust grains inside the chamber in an ethanol solution, in order to generate a flux of particles without aggregations. With this new injection system the following improvements are reached:

1) possibility to vary the flow velocity by acting on the pressure difference between the pre-chamber and the simulation chamber;

2) direct injection of CO_2 and particles to simulate the Martian atmosphere;

3) the avoid of particle losses.

Indeed, the ethanol acts as a protective membrane for particles preventing triboelectric effects that cause aggregates.

The Martian simulation chamber is currently used during the development of the MicroMED for tests and calibrations.

ACKNOWLEDGMENT

This work has been supported by ASI (contract's grant number: 2016/41/H.0). The instrument development was funded and coordinated by ASI under the scientific leadership of INAF-Naples, Italy. The data used in this paper can be accessed upon personal request to the first author (fabio.cozzolino@inaf.it).

References

1. Scaccabarozzi, Diego, et al. "MicroMED, design of a particle analyzer for Mars", *Measurement* 122 (2018): 466-472,
2. Bourke, M. C., K. S. Edgett, and B. A. Cantor (2008), Recent aeolian dune change on Mars, *Geomorphology*, 94, 247–255, doi:10.1016/j.geomorph.2007.05.012.
3. Desch, S.J., Cuzzi, J.N., 2000. The generation of lightning in the solar nebula. Icarus143 (1), 87–105.

4. Drossart, P. et al., "Martian aerosol properties from the Phobos/ISM experiment", Annales Geophysicae 9, 754-760, 1991.
5. Esposito, F., Molinaro, R., Popa, C. I., Molfese, C., Cozzolino, F., Marty, L., ... & Ori, G. G. (2016). The role of the atmospheric electric field in the dust-lifting process. *Geophysical Research Letters*, *43*(10), 5501-5508.
6. Farrell, W.M., McLain, J.L., Collier, M.R., Keller, J.W., 2017. The Martian dust devil electron avalanche: laboratory measurements of the E-field fortifying effects of dust-electron absorption. Icarus297, 90–96.
7. Fedorova, A. A. et al., "Solar infrared occultation observations by SPICAM experiment on Mars-Express: Simultaneous measurements of the vertical distributions of H2O, CO2 and aerosol" Icarus 200, 96-117, 2009. doi:10.1016/j.icarus.2008.11.006
8. Franzese, G., Esposito, F., Lorenz, R., Silvestro, S., Popa, C. I., Molinaro, R., ... & Deniskina, N. (2018). Electric properties of dust devils. *Earth and Planetary Science Letters*, *493*, 71-81.
9. Martínez, G.M., Newman, C.N., De Vicente-Retortillo, A., Fischer, E., Renno, N.O., Richardson, M.I., Fairén, A.G., Genzer, M., Guzewich, S.D., Haberle, R.M. and Harri, A.M., 2017. The modern near-surface Martian climate: A review of in-situ meteorological data from Viking to Curiosity. Space Science Reviews, 212(1-2), pp.295-338.
10. Vicente-Retortillo, Á., G. M. Martínez, N. O. Renno, M. T. Lemmon, and M. de la Torre-Juárez (2017), Determination of dust aerosol particle size at Gale Crater using REMS UVS and Mastcam measurements, Geophys. Res. Lett., 44, doi:10.1002/2017GL072589.
11. Kunkel, W.B., 1950. The static electrification of dust particles on dispersion into a cloud. J. Appl. Phys.21 (8), 820–832.
12. McCarty, L.S., Whitesides, G.M., 2008. Electrostatic charging due to separation of ions at interfaces: contact electrification of ionic electrets. Angew. Chem., Int. Ed. Engl.47 (12), 2188–2207.
13. Melnik, O., Parrot, M., 1998. Electrostatic discharge in Martian dust storms. J. Geo-phys. Res. Space Phys.103 (A12), 29107–29117.

14. Mongelluzzo, G., Esposito, F., Cozzolino, F., Molfese, C., Silvestro, S., Popa, C. I., ... & Scaccabarozzi, D. (2018, June). Optimization of the fluid dynamic design of the Dust Suite-MicroMED sensor for the ExoMars 2020 mission. In 2018 5th IEEE international workshop on metrology for aerospace (MetroAeroSpace) (pp. 134-139). IEEE.
15. Pollack, J. B. et al., "Viking Lander image analysis of Martian atmospheric dust" Journal of Geophysical Research 100, 5235-5250, 1995. doi:10.1029/94JE02640
16. Silvestro, S., Fenton, L. K., Vaz, D. A., Bridges, N. T., & Ori, G. G. (2010). Ripple migration and dune activity on Mars: Evidence for dynamic wind processes. *Geophysical Research Letters*, *37*(20).
17. Silvestro, S., Vaz, D. A., Di Achille, G., Popa, I. C., & Esposito, F. (2015). Evidence for different episodes of aeolian construction and a new type of wind streak in the 2016 ExoMars landing ellipse in Meridiani Planum, Mars. *Journal of Geophysical Research: Planets*, *120*(4), 760-774.
18. Tomasko, M. G. et al., "Properties of dust in the Martian atmosphere from the Imager on Mars Pathfinder" Journal of Geophysical Research 104, 8987-9008, 1999. doi:10.1029/1998JE900016.
19. Toon, O. B. et al., "Physical properties of the particles composing the Martian dust storm of 1971-1972", Icarus 30, 663-696, 1977. doi:10.1016/0019-1035(77)90088-4.
20. Vasilyev, A. V.; Mayorov, B. S.; Bibring, J.-P., “The retrieval of altitude profiles of the Martian aerosol microphysical characteristics from the limb measurements of the Mars Express OMEGA spectrometer”, Solar System Research, Volume 43, Issue 5, pp.392-404, 2009.
21. Zurek, R. W., Barnes, J. R., Haberle, R. M., Pollack, J. B., Tillman, J. E., & Leovy, C. B. (1992). Dynamics of the atmosphere of Mars. *Mars*, 835-933.
22. Harrison et al.2016. *Applications of Electrified Dust and Dust Devil Electrodynamics to Martian Atmospheric Electricity* Space Sci Rev (2016) 203:299–345.

23. Neakrase et Al.,2016. *Particle Lifting Processes in Dust Devils* Space Sci Rev (2016) 203:347–376.

24. Murphy et Al.,2016. *Field Measurements of Terrestrial and Martian Dust Devils* Space Sci Rev (2016) 203:39–87.

25. Newman et Al 2002**.** Modeling the Martian dust cycle, 1. *Representations of dust transport processes* JOURNAL OF GEOPHYSICAL RESEARCH, VOL. 107, NO. E12, 5123**.**

26. Kahre et Al 2006. *Modeling the Martian dust cycle and surface dustreservoirs with the NASA Ames general circulationmodel* JOURNAL OF GEOPHYSICAL RESEARCH, VOL. 111, E06008.

27. Taylor et Al. 2007. *Modelling dust distributions in the atmospheric boundary layer on Mars.* Boundary-Layer Meteorology volume 125, pages305–328(2007).